

Sidelobe suppression in all-fiber acousto-optic tunable filter using torsional acoustic wave

Kwang Jo Lee,^{1,3,4,*} In-Kag Hwang,¹ Hyun Chul Park,² and Byoung Yoon Kim³

¹Department of Physics, Chonnam National University, 300 Yongbong-dong, Buk-gu, Gwangju, 500-757, Korea

²Instrumentation & Control Research Group, POSLAB, 1, Goedong-dong, Nam-gu, Pohang, Gyeongbuk, 790-300, Korea

³Department of Physics, Korea Advanced Institute of Science and Technology, 373-1 Guseong-dong, Yuseong-gu, Daejeon, 305-701, Korea

⁴Currently with the Optoelectronics Research Centre, University of Southampton, Southampton, SO17 1BJ, UK

* kjl@kaist.ac.kr

Abstract: We propose two techniques to suppress intrinsic sidelobe spectra in all-fiber acousto-optic tunable filter using torsional acoustic wave. The techniques are based on either double-pass filter configuration or axial tailoring of mode coupling strength along an acousto-optic interaction region in a highly birefringent optical fiber. The sidelobe peak in the filter spectrum is experimentally suppressed from -8.3dB to -16.4dB by employing double-pass configuration. Axial modulation of acousto-optic coupling strength is proposed using axial variation of the fiber diameter, and the simulation results show that the maximum side peak of -9.3dB can be reduced to -22.2dB . We also discuss the possibility of further spectral shaping of the filter based on the axial tailoring of acousto-optic coupling strength.

©2010 Optical Society of America

OCIS codes: (060.2310) Fiber optics; (230.1040) Acousto-optical devices.

References and links

1. H. S. Kim, S. H. Yun, I. K. Kwang, and B. Y. Kim, "All-fiber acousto-optic tunable notch filter with electronically controllable spectral profile," *Opt. Lett.* **22**(19), 1476–1478 (1997).
 2. K. J. Lee, D.-I. Yeom, and B. Y. Kim, "Narrowband, polarization insensitive all-fiber acousto-optic tunable bandpass filter," *Opt. Express* **15**(6), 2987–2992 (2007).
 3. M. Berwick, C. N. Pannell, P. St. J. Russell, and D. A. Jackson, "Demonstration of birefringent optical fibre frequency shifter employing torsional acoustic waves," *Electron. Lett.* **27**(9), 713–715 (1991).
 4. K. J. Lee, H. C. Park, and B. Y. Kim, "Highly efficient all-fiber tunable polarization filter using torsional acoustic wave," *Opt. Express* **15**(19), 12362–12367 (2007).
 5. K. J. Lee, K. S. Hong, H. C. Park, and B. Y. Kim, "Polarization coupling in a highly birefringent photonic crystal fiber by torsional acoustic wave," *Opt. Express* **16**(7), 4631–4638 (2008).
 6. K. J. Lee, I.-K. Hwang, H. C. Park, and B. Y. Kim, "Polarization-coupling all-fiber acousto-optic tunable filter insensitive to fiber bend and physical contact," *Opt. Express* **17**(8), 6096–6100 (2009).
 7. K. J. Lee, I.-K. Hwang, H. C. Park, and B. Y. Kim, "Polarization independent all-fiber acousto-optic tunable filter using torsional acoustic wave," *IEEE Photon. Technol. Lett.* **22**(8), 523–525 (2010).
 8. K. J. Lee, I.-K. Hwang, H. C. Park, K. H. Nam, and B. Y. Kim, "Analyses of unintentional intensity modulation in all-fiber acousto-optic tunable filters," *Opt. Express* **18**(5), 3985–3992 (2010).
 9. H. C. Park, B. Y. Kim, and H. S. Park, "Apodization of elliptical-core two-mode fiber acousto-optic filter based on acoustic polarization control," *Opt. Lett.* **30**(23), 3126–3128 (2005).
 10. D. O. Culverhouse, S. H. Yun, D. J. Richardson, T. A. Birks, S. G. Farwell, and P. S. J. Russell, "Low-loss all-fiber acousto-optic tunable filter," *Opt. Lett.* **22**(2), 96–98 (1997).
 11. D. A. Satorius, T. E. Dimmick, and G. L. Burdge, "Double-pass acoustooptic tunable bandpass filter with zero frequency shift and reduced polarization sensitivity," *IEEE Photon. Technol. Lett.* **14**(9), 1324–1326 (2002).
 12. A. Kar-Roy, and C. S. Tsai, "Low-sidelobe weighted-coupled integrated acoustooptic tunable filter using focused surface acoustic waves," *IEEE Photon. Technol. Lett.* **4**(10), 1132–1135 (1992).
 13. D. A. Smith, and J. J. Johnson, "Sidelobe suppression in an acousto-optic filter with a raised-cosine interaction strength," *Appl. Phys. Lett.* **61**(9), 1025–1027 (1992).
 14. H. E. Engan, "Analysis of polarization-mode coupling by acoustic torsional waves in optical fibers," *J. Opt. Soc. Am. A* **13**(1), 112–118 (1996).
 15. B. Langli, and K. Bløtekjær, "Effect of acoustic birefringence on acoustooptic interaction in birefringent two-mode optical fibers," *J. Lightwave Technol.* **21**(2), 528–535 (2003).
-

1. Introduction

Tunable optical filters are key components in optical communication networks and sensor systems. In particular, all-fiber acousto-optic tunable filters (AOTFs) have attracted considerable interest due to their advantages including low insertion loss, wide and fast wavelength tuning, low polarization dependence, and variable attenuation via simple electronic control [1–4]. The all-fiber AOTFs have been demonstrated based on wavelength selective acousto-optic (AO) mode coupling by traveling flexural [1, 2] or torsional acoustic waves [3, 4]. In these devices, the acoustic waves produce the resonant coupling between two spatial modes in an optical fiber (for flexural wave) or between two polarization modes in a highly birefringent (HB) fiber (for torsional wave). The recently developed torsional mode AOTF has several important advantages above the flexural wave counterpart. They include simple switching between notch and bandpass filter types [4], no acoustic birefringence [5], immunity to external perturbation such as physical contact or fiber bending [6], polarization independent operation [7], and relatively low intensity fluctuation [8].

However, the torsional mode AOTF still suffers from intrinsic sidelobes (with a theoretical peak level of -9.3dB) on both sides of the main filtering band. In various optical systems, sharp and well defined filter responses are crucial, and such undesirable sidelobes introduce crosstalk between adjacent channels in wavelength-division-multiplexed (WDM) systems. There have been several approaches proposed to suppress the sidelobes in all-fiber flexural mode AOTFs [9–11] and integrated-optic AOTFs [12, 13]. They fall in one of two categories of axial variation of coupling strength (apodization) [9, 12, 13] and double-pass of the light through the device [10, 11]. In reference [9], fiber twisting technique was applied to the flexural mode AOTF in order to modulate the AO coupling strength between two spatial modes in an elliptical-core fiber at the given acoustic frequency. However, this technique does not work in the case of our torsional mode counterpart since the torsional mode AOTF is based on coupling between two polarization modes, not between the spatial modes. The flexural mode AOTF with the double-pass configuration requires a mode-selective coupler (MSC) to separate two interacting spatial modes [10, 11], but its complicated fabrication process and strong wavelength dependence make this approach not attractive. Acoustic amplitude apodization technique used for the integrated-optic AOTFs cannot be easily applied to fiber counterparts due to the difficulty in controlling the acoustic wave amplitude profile along a freestanding fiber [12, 13].

In this paper, we show that both the apodization and the double-pass techniques can be applied to torsional mode AOTF more effectively, thanks to the special features of the device. The device is reconfigured for double-pass scheme by adding a mirror and a circulator (or a polarization beam splitter), and the apodization is realized by varying the fiber diameter along the AO interaction length. The experimental results using the double-pass scheme is compared with the theoretical predictions. We also discuss the possibility of designing spectral shape of the filter by the axial tailoring of AO coupling strength.

2. Sidelobe suppression based on a double-pass filter configuration

Multiple passes through the all-fiber AOTFs are a useful technique to obtain lower sidelobe spectra and narrower bandwidth as long as they have low insertion loss [10, 11]. In the torsional mode AOTF, the double-pass configuration is prepared by placing a mirror at the end of the fiber and using a circulator to receive the filter output. In contrast to the case of the flexural mode counterpart, which is based on the coupling between two spatial modes, the device structure is much simpler because the polarization modes can be easily manipulated using commercial polarizer instead of the MSC.

The schematic of the proposed filter structure is illustrated in Fig. 1. The device is composed of a torsional acoustic transducer, a high-reflection (HR) mirror, a circulator, two polarizers, and a HB fiber. The cross-section of an elliptical core HB fiber used in the experiment is shown in the inset of Fig. 1. The HB fiber has an elliptical core of $2\text{ }\mu\text{m} \times 4\text{ }\mu\text{m}$ dimension, and the outer diameter and the polarization beatlength near 1550 nm are $80\text{ }\mu\text{m}$

and 1.36 mm, respectively. The input polarization state of the LP_{01} mode is aligned to one of the polarization eigenstate using the in-line fiber polarizer, and passes through the circulator. The torsional acoustic wave was generated by the combination of two shear mode lead zirconate titanate (PZT) plates [4]. The 82 cm-long bare fiber for AO interaction was necessary for narrow bandwidth (~ 2 nm) of the filter, which was coiled in the diameter of 5 cm as shown in Fig. 1 [6]. The generated torsional acoustic wave was coupled to a bare section of the fiber bonded to the central hole in the acoustic horn, and was absorbed by an acoustic damper at the end of the AO interaction region. The torsional acoustic wave provides complete coupling between two eigen-polarizations at a resonant wavelength satisfying the phase matching condition [4]. Because the coupled polarization mode can be selected or removed by adjusting the polarization direction of the output polarizer, the AOTF can be operated as the notch type or the bandpass type as illustrated in Fig. 1 [4].

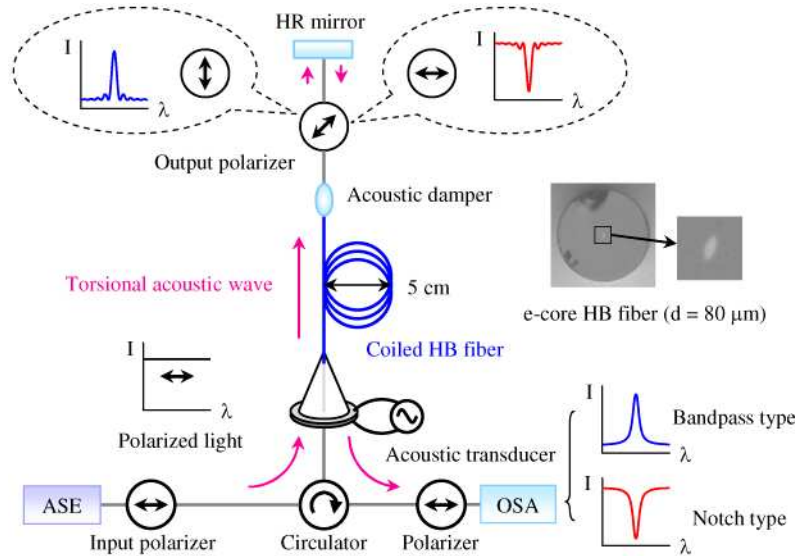


Fig. 1. Schematic of a proposed all-fiber torsional mode AOTF with the double-pass configuration. The inset shows the cross-section of the elliptical core HB fiber used in this experiment. ASE: amplified spontaneous emission source, OSA: optical spectrum analyzer.

First, the device was operated as the bandpass type in a single-pass configuration without the HR mirror. In this case, a horizontally-polarized input light is converted to a vertically-polarized light at the AO phase matching wavelength, so that the single-pass filter output has an orthogonal polarization state because only the converted polarization state can be selected by the output polarizer. The corresponding filter spectra calculated and measured at the end of the polarizer were shown in Fig. 2(a). The maximum value of the side peak was -8.3dB , which is slightly higher than the theoretical value of -9.3dB . The asymmetry in the sidelobe spectra is mainly caused by the small axial non-uniformity in the optical birefringence (or polarization beatlength) [5]. Next, in order to modify the device structure into the double-pass configuration, we attached the HR mirror at the end of the fiber so that the light reentered the AO interaction region. Then the optical output which passes through the final polarizer is detected at the third port of the circulator. In contrast to the single-pass configuration, the double-pass filter output has the same horizontal polarization state because the vertically-polarized light reflected at the mirror passes through the AO coupling region again and thus experiences the AO coupling once more. The final transmission spectrum shows the multiplication of the original spectrum by itself, resulting in sidelobe suppression and bandwidth reduction. Figure 2(b) shows the transmission spectra when the device was operated in the double-pass configuration at the applied acoustic frequency of 2.748 MHz. The experimental result shows that the magnitude of the largest sidelobe was reduced from

−8.3dB to −16.4dB in the double-pass configuration. The complete coupling between two polarization modes was achieved, and the measured 3-dB optical bandwidth was reduced from 2.3 nm to 1.9 nm by a factor of 0.83 (theoretical ratio = 0.73) by introducing the double-pass scheme. The dotted curves in Figs. 2(a) and 2(b) represent the spectral responses calculated for uniform coupling strength in the AO interaction region.

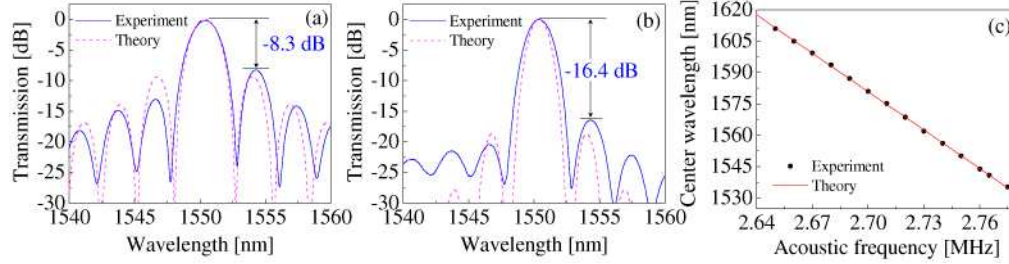


Fig. 2. Experimental and theoretical transmission spectra of the all-fiber torsional mode AOTF (a) with the single-pass and (b) with the double-pass configurations at the applied acoustic frequency of 2.748 MHz. (c) Center wavelength of the filter plotted as a function of the applied acoustic frequency.

Figure 2(c) shows the wavelength tuning property of the device with the double-pass configuration. The center wavelength was plotted as a function of the applied acoustic frequency, which could be linearly and continuously tuned over the whole wavelength range of 1530 - 1620 nm (limited by the light source) by a change of only 5% in the acoustic frequency. In contrast to the flexural mode counterpart with the MSC, the wavelength tuning range of the all-fiber torsional mode AOTF is not affected by the device configurations (single- or double-pass), as we described above.

3. Sidelobe suppression based on axial tailoring of the AO coupling strength

Apodization of the AO coupling strength (and therefore the filter spectrum) can be readily available for the all-fiber torsional mode AOTF based on a few interesting features of the torsional acoustic wave. One is that the AO coupling strength is inversely proportional to the square of the fiber diameter [14]. Another is that the wavelength of the lowest order torsional acoustic mode used for the AO coupling is independent of the fiber diameter [14]. If the outer diameter of the HB fiber is varied along the fiber length without modifying the polarization beatlength, the coupling strength varies along the fiber for a fixed resonant wavelength. In contrast, the axial variation of the fiber diameter induces a wavelength chirp in the flexural acoustic wave along the AO interaction region, which changes the phase matching condition in the flexural mode AOTF. Also a small non-circularity of the fiber cross-section, which can be accompanied by the diameter change, introduces the acoustic birefringence for the flexural wave, resulting in complexity in output filter spectrum [15].

Figure 3(a) illustrates the axial variation of the fiber diameter along the HB fiber. As the simplest example, if we consider the axial diameter profile as a quadratic function shape with respect to distance from the center of the AO interaction region, the axial variation of the fiber diameter $[d(z)]$ can be expressed as follows:

$$\frac{d(z)}{d_0} = \frac{4}{L^2}(1-m)z(z-L) + 1. \quad (1)$$

Here, d_0 , L , and m denote the initial fiber diameter, the AO interaction length, and the normalized fiber diameter at the center of the AO interaction region, respectively. In this case, the AO coupling coefficient which is inversely proportional to the square of the fiber diameter is also expressed as,

$$\kappa(z) = \kappa_0 \left[\frac{d(z)}{d_0} \right]^{-2}, \quad (2)$$

where, κ_0 denote the initial coupling coefficient, and it is given by $\pi/2L$ for complete coupling between two interacting polarization modes in a un-modified fiber. Then the coupled mode equations describing the AO mode coupling are expressed as follows:

$$\frac{dA_x(z)}{dz} = -i\kappa(z)A_y(z)e^{i\beta z}, \quad (3)$$

$$\frac{dA_y(z)}{dz} = -i\kappa(z)A_x(z)e^{-i\beta z}. \quad (4)$$

Here, $A_x(z)$ and $A_y(z)$ denote the normalized complex electric fields of two interacting polarization modes, respectively. The wavelength dependent phase mismatch is given by,

$$\beta \equiv 2\pi \left(\frac{1}{L_B(\lambda)} - \frac{1}{\Lambda} \right), \quad (5)$$

where, L_B and Λ denote the optical beatlength between two polarization modes and the applied acoustic wavelength, respectively. The coupled-mode equations in Eq. (3) and (4) were numerically solved by considering the same parameters for the HB fiber that we used in the experiments described in the previous section.

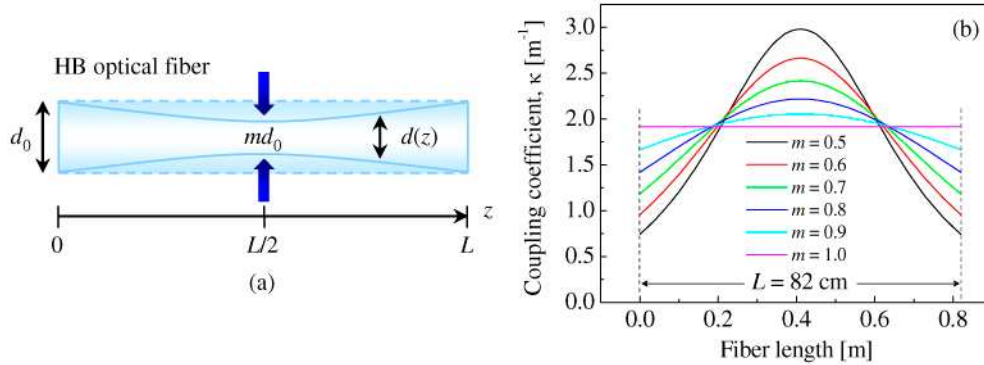


Fig. 3. (a) Variation of the fiber diameter along the AO interaction region. m : normalized fiber diameter at the center of the AO interaction region, L : AO interaction length for complete mode coupling. (b) Axial variation of the AO coupling coefficient plotted as a function of the fiber length for each m -value.

The calculated AO coupling coefficients [Eq. (2)] are plotted in Fig. 3(b) as a function of the fiber length for several m -values, which indicate that the AO coupling strength is modulated by the diameter change along the fiber. The AO interaction length for complete mode coupling was maintained at 82 cm for each m -value, and then the acoustic drive power required for the complete mode coupling decreases with decreasing m -value. In this case, the areas under each curve remain constant for different m -values. As can be seen in Fig. 3(b), the AO coupling coefficients for $m < 1$ have the minimum values at both ends of the interaction region and the maximum values in the middle. The shape of the coupling coefficient variation approaches to an ideal Gaussian shape with decreasing m -value, which means that the sidelobe suppression will be also improved with decreasing m -value.

The spectral response of the all-fiber torsional mode AOTF calculated for each m -value is shown in Fig. 4(a). The series of sidelobe in the filter spectrum were suppressed for $m < 1$ as expected above, and the maximum value of intrinsic side peak could be reduced from -9.3 dB

to -22.2dB at $m = 0.5$. This value is smaller than -18.6dB which is theoretically achievable in the double-pass scheme with uniform coupling strength [see Fig. 2(b)]. This suggests that the axial tailoring of the coupling strength is more efficient technique as compared to the case of the double-pass scheme. However, this approach results in broadening of the filter bandwidth due to the reduction of the effective AO interaction length, while bandwidth narrowing was observed in the double-pass scheme. The variation of the maximum side peak was plotted in Fig. 4(b) as a function of the m -value, showing that the sidelobe suppression can be improved at the smaller m -value. The results shows that the sidelobe spectra can be further suppressed below -44.4dB ($-22.2\text{dB} \times 2$) by use of the apodization technique at $m = 0.5$ in the double-pass scheme. If the m -value becomes smaller than 0.5, the main peak starts to merge the side peaks due to the broadening of main filtering band, resulting in both poor filter extinction ratio and deterioration in the filter spectrum.

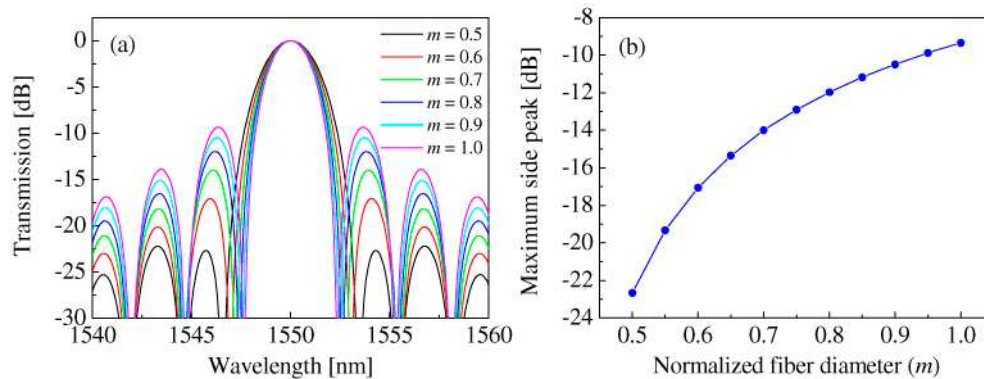


Fig. 4. (a) Spectral response of the all-fiber torsional mode AOTF calculated for each m -value, and (b) the maximum side peak in the filter spectrum plotted as a function of the m -value.

The axial modulation of the coupling strength by the diameter change along the HB fiber is a promising technique to design the spectral shape of the all-fiber torsional mode AOTF. For example, either a rectangular- or a Gaussian-shaped filter spectrum which is frequently used in various optical systems can be tailored using this technique.

4. Conclusion

In conclusion, we have described two efficient techniques to suppress the sidelobe spectra in all-fiber torsional mode AOTF. The theoretical and the experimental results showed that the maximum sidelobe could be suppressed to -22.2dB and -16.4dB by using the axial modulation of the AO coupling strength and the double-pass device configuration, respectively. When combining the two techniques, the sidelobe suppression below -40dB can be achieved. We believe that the spectral design technique using the axial tailoring of mode coupling strength in the all-fiber torsional mode AOTF has a great potential and will find diverse applications in optical communication and sensor systems.

Acknowledgement

This work was supported by the Regional Research Center for Photonic Materials and Devices, Chonnam National University, and the Korea Research Foundation Grant funded by the Korean Government (MOEHRD, Basic Research Promotion Fund) (KRF-2008-331-C00115).